



Pulsed electric fields (PEF) treatment to enhance starch 3D printing application: Effect on structure, properties, and functionality of wheat and cassava starches

Bianca Chiericato Maniglia, Gianpiero Pataro, Giovanna Ferrari, Pedro Esteves Duarte Augusto, Patricia Le-Bail, Alain Le-Bail

► To cite this version:

Bianca Chiericato Maniglia, Gianpiero Pataro, Giovanna Ferrari, Pedro Esteves Duarte Augusto, Patricia Le-Bail, et al.. Pulsed electric fields (PEF) treatment to enhance starch 3D printing application: Effect on structure, properties, and functionality of wheat and cassava starches. Innovative Food Science & Emerging Technologies / Innovative Food Science and Emerging Technologies , 2021, 68, pp.102602. 10.1016/j.ifset.2021.102602 . hal-03127178

HAL Id: hal-03127178

<https://hal.inrae.fr/hal-03127178>

Submitted on 3 Feb 2023

HAL is a multi-disciplinary open access archive for the deposit and dissemination of scientific research documents, whether they are published or not. The documents may come from teaching and research institutions in France or abroad, or from public or private research centers.

L'archive ouverte pluridisciplinaire **HAL**, est destinée au dépôt et à la diffusion de documents scientifiques de niveau recherche, publiés ou non, émanant des établissements d'enseignement et de recherche français ou étrangers, des laboratoires publics ou privés.



Distributed under a Creative Commons Attribution - NonCommercial 4.0 International License

Pulsed electric fields (PEF) treatment to enhance starch 3D printing application: effect on structure, properties, and functionality of wheat and cassava starches

Bianca Chieregato Maniglia^{a,b,c,f,*}, Gianpiero Pataro^d, Giovanna Ferrari^{d,e}, Pedro Esteves Duarte Augusto^{f,g}, Patricia Le-Bail^{b,c}, Alain Le-Bail^{a,b,c,*}

^a ONIRIS-GEPEA UMR CNRS 6144 Nantes - France

^b BIA-INRAe UR 1268 Nantes – France

^c SFR IBSM INRA CNRS 4202

^d Department of Industrial Engineering, University of Salerno (UNISA), Via Giovanni Paolo II, 132-84084, Fisciano, SA – Italy

^e ProdAl Scarl, University of Salerno, via Ponte don Melillo, 84084 Fisciano, SA, Italy

^f Department of Agri-food Industry, Food, and Nutrition (LAN), Luiz de Queiroz, College of Agriculture (ESALQ), University of São Paulo (USP), Piracicaba, SP – Brazil

^g Food and Nutrition Research Center (NAPAN), University of São Paulo (USP), São Paulo, SP, Brazil

*biancamaniglia@usp.br; *alain.lebail@oniris-nantes.fr

ABSTRACT

This work evaluated the impact of PEF on the structure, properties, and functionality of wheat and cassava starches focusing on 3D printing application. Aqueous starch suspensions were PEF-treated using three different combinations of field strength and total specific energy input (T1:15 kV/cm;25 kJ/kg; T2:25 kV/cm;25 kJ/kg; and T3:25 kV/cm;50 kJ/kg). The three conditions had the same effect on cassava starch (no damage on granules surface, reduction of peak apparent viscosity, firmer gels), while T3 promoted a greater effect on wheat starch (fractures on granules surface, reduction in peak apparent viscosity, and firmer gels). T3 condition was selected for further evaluation, revealing depolymerization, reduction of relative crystallinity, and gelatinization enthalpy, but no changes in functional groups. PEF-treated wheat starch resulted in 3D printing with a smoother surface and different texture, while PEF-treated cassava starch showed the same performance of native starch. Therefore, PEF affects differently each source, potentially enhancing 3D printing applications.

Keywords: starch modification, pulsed electric field, gelatinization, additive manufacturing, 3D printing, printability.

1. Introduction

Starch has been extensively applied in different sectors like food, textile, paper, chemical, pharmaceutical, and petrochemical industries. However, this polysaccharide presents limited functionalities in its native form, which can hinder its applications. As a result, several methods have been applied to induce a targeted modification in order to improve the technological and functional properties of starch. Although chemical modification methods are the most applied industrially, there is an increasing concern regarding their use (Maniglia, Castanha, Le-Bail, Le-Bail, & Augusto, 2020), which are motivating scientists to explore innovative methods based on the application of emerging technologies (Maniglia, Castanha, Rojas, & Augusto, 2020).

In this scenario, pulsed electric field (PEF) is an emergent physical method that has been used to decontaminate food product, improve extractions, fermentation, dehydration, peeling, and softening processes (Arnal et al., 2018; Raso et al., 2016; Zhu, 2018). Apart from these applications, PEF method could affect the functional properties of biomacromolecules, such as polysaccharides and proteins (Giteru, Oey, & Ali, 2018).

In this regard, recent studies have indicated PEF treatments can affect starch conformation, microstructure, particle size, viscoelastic properties, solubility, swelling effect, *in vitro* digestibility, structural transition, and thermal stability (Abduh, Leong, Agyei, & Oey, 2019). Compared to other methods for starch modification, PEF shows the advantage of inducing the changes in physicochemical properties of starch with less energy for a short period (Zhu, 2018).

The modified starches produced by emerging technologies can achieve different functionality, which could be exploited, among others, to enhance 3D printing. The latter is an innovative method that can produce materials with freedom in design and customization, with a personalized and intricate shape and internal structure (Mantihal, Kobun, & Lee, 2020).

Starch-based materials for 3D printing application have been investigated for different uses, from food to medicine (Fanli Yang, Min Zhanga, Bhesh Bhandari, 2018; Koski & Bose, 2019). However, there is still a limited number of studies producing modified starches for 3D printing, but, to date, none of them focused on the use of PEF-treated starch.

The main objective of this work was to assess the potential of PEF treatment to induce targeted modifications on starch in order to improve its 3D printability.

For this work, wheat and cassava starches were chosen since they are among the most used starch sources in the food, paper, and chemical engineering industries (Pourmohammadi, Abedi, Hashemi, & Torri, 2018; Shevkani, Singh, Bajaj, & Kaur, 2017),

Firstly, the effect of different combinations of field strength (E) and total specific energy input (W_T) on granule morphology, chemical-physical, thermal and textural properties of starch was investigated. PEF processing conditions enabling to obtain modified starches with the capacity to produce stronger hydrogels was selected for this work, since this property is associated with a better printability. Then, under the selected PEF treatment conditions, the potential of the modified starches for 3D printing applications was evaluated, evaluating the definition, reproducibility, and texture of the printed samples based on modified starch hydrogels.

2. Material and methods

2.1. Raw material and sample preparation

Native cassava starch (Amilogill 1500) was supplied by Cargill Agrícola – Brazil (moisture content of 13.2 g/ 100 g). Native wheat starch (CAS 9005-25-8) was obtained from Merck KGaA (Germany) (moisture content of 10.1 g/ 100 g). All the chemicals were of analytical grade.

Before processing, suspensions of either wheat or cassava starch were prepared by adding the starch powder to distilled water up to a final concentration of 8% (w/v). The initial electrical conductivity of starch suspensions (0.089 ± 0.003 Ms/cm at 25°C, on average) (Conductivity-meter HI 9033, Hanna Instrument, Milan, Italy) was adjusted by adding a given amount of KCl up to a final value of about 1 Ms/cm at 25°C, which ensured better performance of the PEF system used for the experiments.

2.2. PEF treatment

PEF treatments were conducted in a bench-scale continuous flow PEF unit (Fig. 1) previously described in detail by Postma et al. (2016) and Carullo et al. (2018), with some modifications. Briefly, it consisted of a peristaltic pump used to transfer the starch suspensions through a stainless steel coiled tube submerged into a water heating bath used to control the inlet temperature to the treatment chamber. The latter consisted of two modules, each one made of two co-linear cylindrical treatment chambers, hydraulically connected in series, with an inner radius of 1.25 mm and a gap distance of 4 mm. The treatment chambers were connected to the output of a high voltage pulsed power (20 kV–100 A) generator (Diversified Technology Inc., Bedford, WA, USA) able to deliver monopolar square pulses (1–10 μ s, 1–1000 Hz). The maximum electric field intensity (E , in kV/cm) and total specific energy input (W_T , in kJ/kg suspension) were calculated as reported by Postma et al. (2016). T-thermocouples were used to measure the product temperature at the inlet and outlet of each module of the PEF chamber.

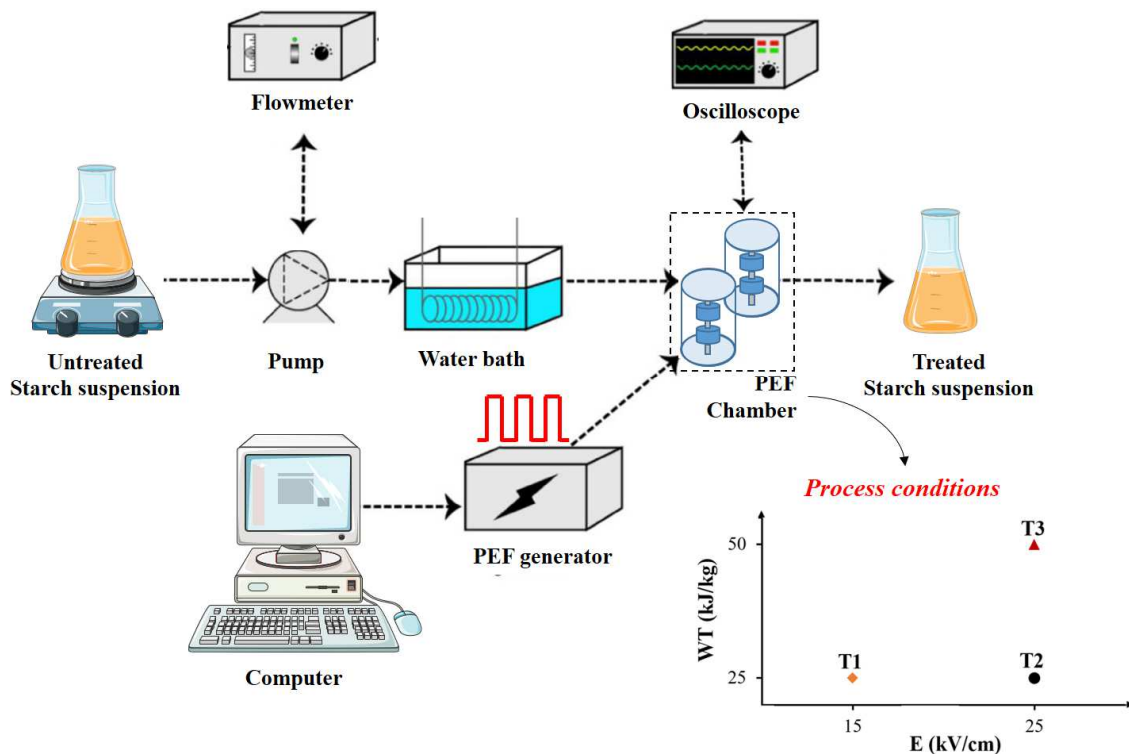


Fig. 1. Schematic of continuous flow PEF system (E : electric field strength, W_T : total specific energy input; T1, T2, and T3: processing conditions).

During PEF treatment, the starch suspension was pumped, from a feeding tank under stirring, through the treatment chamber at a constant flow rate of 2 L/h. In all the experiments, the pulse length was fixed at 5 μ s, while the electric field strength and total specific energy input were set by varying the applied voltage and the pulse repetition frequency, respectively. First, three different combinations of field strength and energy input (T1: 15 kV/cm - 25 kJ/kg; T2: 25 kV/cm - 25 kJ/kg; and T3: 25 kV/cm - 50 kJ/kg) were selected to treat both wheat (W) and cassava (C) starches, as depicted in Fig. 1 and Table 1. All the experiments were carried out at an inlet temperature of each module of PEF chamber of $25 \pm 2^\circ\text{C}$, while the maximum temperature increase of the samples, detected at the exit of the treatment chamber, never exceeded 10°C .

For the sake of comparison, untreated (control) samples of the starch suspensions were pumped through the PEF plant with the heating bath set at 25°C , but with the PEF generator switched off.

At the exit of the treatment chamber, untreated (control) and PEF treated suspensions were collected in plastic tubes and placed in an ice-water bath to be rapidly cooled up to a final temperature of 25°C before undergoing the aqueous extraction process.

After processing, the starch suspension was collected and maintained at rest for decanting. After 18 h, the supernatant was discarded while the starch was recovered and dried in an air circulation oven (Heraeus, Germany) at 35°C until reaching a moisture content of approximately 12%. The dried starch was then macerated, sieved ($250 \mu\text{m}$), and stored in glass containers until further analysis.

The untreated and PEF-treated samples were named as reported in Table 1.

Table 1. Treatment labels of untreated and PEF-treated samples.

Starch source	Control (without treatment)	T1 (15 kV/cm; 25 kJ/kg)	T2 (25 kV/cm; 25 kJ/kg)	T3 (25 kV/cm; 50 kJ/kg)
Cassava	C_Control	C_T1	C_T2	C_T3
Wheat	W_Control	W_T1	W_T2	W_T3

2.3. Starch characterization

2.3.1. Granule morphology

The starch granules morphology of untreated and PEF-treated starch samples was observed using a Nikon Eclipse TE2000-U light microscope (Nikon, UK) with a magnification of 20 x and a digital camera of 5.1 megapixels (MT9P001, Aptina, Colorado, USA). The starch granules were dispersed in distilled water (1:1, v/v). Then, they were placed on a glass slide, covered by a glass coverslip, and analysed. For determination of birefringence, the samples were examined with the same microscope but equipped with a crossed polarizing filter.

2.3.2 Molecular characterization: pH, functional groups, molecular size distribution, and apparent amylose content

pH values were measured in the starch suspension of 10.7% (w/w) in distilled water, under constant stirring at room temperature (25°C), using a potentiometer (model TEC-5 mode, Tecnal, Piracicaba, Brazil).

The changes in the functional groups were evaluated using Fourier transform infrared (FTIR) spectroscopy through Spectrum 100™ FTIR instrument (Perkin-Elmer, Shelton, USA) equipped with an attenuated total reflection (ATR) accessory. All the spectra were the average of 16 scans in the range from 4000 cm⁻¹ to 650 cm⁻¹, which were acquired at a resolution of 4 cm⁻¹.

The molecular size distribution profile was determined using a gel permeation chromatography (GPC) system, according to Song & Jane (2000), with some modifications. Starch samples (0.1 g, on dry basis) were dispersed in 10 mL of 90% dimethylsulfoxide (Labsynth, Brazil), heated in a water-bath set at 100°C for 1 h and then kept at 25°C for 16 h under constant stirring. Afterward, an aliquot of 3 mL of the suspension was mixed with 10 mL of absolute ethanol and centrifuged for 30 min at 3000 g. The precipitated starch was then dissolved in 9 mL of distilled water, placed in a water-bath set at 100°C for 30 min. An aliquot of 4 mL was then upwardly eluted in the chromatographic column (GE XK 26/70, 2.6 cm diameter x 70 cm high) packed with Sepharose CL-2B gel (Sigma, Sweden), with an eluent solution (25 mmol/L of NaCl and 1

mmol/L of NaOH), at a rate of 60 mL/h. A fraction collector (Gilson, model FC203B, Middleton, England) separated fractions of 4 mL of the eluted solution in different tubes. The samples were then evaluated by the blue value method (Juliano, 1971), using a spectrophotometer at a wavelength of 620 nm (Spectrometer Femto, Model 600S, São Paulo, Brazil).

2.3.3 Thermal and crystalline properties

The thermal properties during starch gelatinization were determined using a Multi-Cell Differential Scanning Calorimeter (MC-DSC) – (TA Instruments, Lindon, Utah, USA). The starch samples were weighed and hydrated directly into the ampoules (10 g starch / 100 g suspension). An ampoule with deionized water was used as a reference and three runs for each sample were analyzed. The MC-DSC heating program consisted of going from 20 to 100°C at a rate of 2°C/min. The onset temperature (T_o), the peak temperature (T_p), the final temperature (T_f), and the gelatinization enthalpy (ΔH) associated with the starch gelatinization interval were calculated using the Universal Analyser software (TA Instruments).

The relative crystallinity of starch powder was determined by X-ray diffraction (XRD) Inel X-ray equipment (Inel, France) operated at 40 kV and 30 mA. The Cu $K\alpha$ radiation (0.15405 nm) was selected using a quartz monochromator. Before the XRD analysis, the starch samples were maintained in a desiccator containing a saturated $BaCl_2$ solution (25°C, $a_w = 0.900$) for 7 days to ensure constant water activity. Diffracted intensities were monitored (2θ) by a sensitive detector (CPS 120, Inel, France). The resulting diffraction diagrams were normalized between 3° and 30° (2θ). The curves obtained were smoothed using the Origin software, version 2018 (Microcal Inc., Northampton, MA, USA). The relative crystallinity was calculated as the ratio of upper diffraction peak area to the total diffraction area, following the method described by Nara & Komiya (1983) and considering 2θ ranging from 3° to 30°.

The thermal and crystalline properties were analyzed in triplicates.

2.3.4. Pasting properties and texture profile of hydrogels

Hydrogels pasting properties were determined using a TA AR2000 rheometer (TA Instruments, New Castle, DE) equipped with a starch pasting cell attachment. Starch suspensions at 10.7 g starch / 100 g (corrected to 14 % moisture basis) were prepared and evaluated through the procedure: heating at 50 °C for 1 min, then heating at 95 °C (6 °C/min) for 5 min and after that, it was cooled to 50 °C (6 °C/min), and finally, it was kept at 50 °C for 2 min. Different pasting parameters were obtained: peak apparent viscosity – PAV, trough apparent viscosity – TAV, final apparent viscosity – FAV, breakdown – BD, setback – SB, and pasting temperature – PT. The BD represents the absolute difference between the PAV and the TAV. Once both PAV and TAV values are changing at the same time, it can lead to a misinterpretation of the BD values. The same occurs for the SB, which represents the absolute difference between FAV and PAV values, and these parameters are also changing at the same time. Therefore, for a better interpretation of the results, the relative breakdown – RBD (ratio between the BD and PAV values) and the relative setback – RSB (ratio between the SB and TAV values) were calculated. RBD can be associated with the facility of starch granules disruption and RSB can be associated with the retrogradation tendency of the gel (Maniglia, Lima, da Matta Júnior et al., 2020).

Hydrogels were prepared from starch suspensions (10.7 g dry starch/100 g, starch mass corrected to 14% moisture basis) placed in Erlenmeyer flasks and then heated in a water bath at 85 ± 2 °C for 20 min. The hydrogels were placed in plastic cups (40 mm diameter × 20 mm height), kept in a desiccator with water at the bottom to ensure uniform moisture, and stored for 24 h in the refrigerator (5 ± 2 °C) for gelling. The obtained hydrogels were evaluated concerning their firmness by a puncture assay using a texture analyzer TA TX Plus (Stable Micro Systems Ltd., Surrey, UK) with a load cell of 50 kgf (490.3 N). The samples were penetrated until a distance of 4 mm using a cylindrical probe (P/0.5R, 0.5 in of diameter) at $1 \text{ mm} \cdot \text{s}^{-1}$. The equipment measured the force as a function of penetration depth. Hydrogel firmness was evaluated by the energy required to penetrate the material (calculated by the area below the curve: force versus distance of penetration).

2.4. 3D printing process

The starch hydrogels, produced as described in Section 2.3, were transferred into the printer syringes (60 mL), cooled to room temperature, and stored under refrigerated conditions ($5 \pm 2^\circ\text{C}$) for 24 h before printing. Afterward, the printing process was carried out in a 3D printer Stampante 3D (3DRAG V1.2, Futura Elettronica, Italy). A nozzle (0.8 mm diameter x 18 mm height) was coupled to the syringe, the robotic arm showed a velocity of 5 mm/s, and the extrusion rate was 4.5 mg/s at room temperature ($20 \pm 2^\circ\text{C}$). Three different physical shapes (heart, star, and cylinder) were printed using the Repetier Host V2.0.1 and Slic3r software (Hot-World GmbH & Co. KG, Willich, Germany). The dimensions of the heart shape: 5 cm x 6 cm x 2 mm (Length x Width x Height), star shape: 2.5 cm x 2.5 cm x 2 mm (Length x Width x Height), and cylinder shape: 2 cm x 4 cm (diameter x height). Five samples for each starch hydrogel and shape were printed.

The printed cylinders were conditioned in a refrigerator ($5 \pm 2^\circ\text{C}$) for 24 h and then placed inside a desiccator with water to avoid dehydration, before being subjected to texture profile analysis (TPA). The analyses were conducted in triplicates for each sample using a texture analyser TA-XT+ (Stable Microsystems, Surrey, UK). The TPA measurement consisted of two compression-decompression cycles separated by a time interval of 10 s, at a rate of 1 mm/s, using a 25 mm of diameter cylinder probe (Code P/25, Stable Microsystem Ltd.). The probe compressed the sample to 25 % (6.25 cm) of the initial height (25 mm) before decompression using a load cell of 50 kgf (490.3 N). All the textural parameters were measured and calculated by the instrument software from the resulting force-deformation curves, including hardness, adhesiveness, cohesiveness, springiness, and chewiness.

The reproducibility of 3D printed samples was evaluated considering the coefficient of variation ($\text{CV} = \text{standard deviation} / \text{mean} \times 100$) of the weight and the dimensions (diameter and height) of the 3D printed cylinders. The samples were weighed in an analytical balance (AZ214, Sartorius, Göttingen, Germany) and the sizes were measured in five different positions using a digital pachymeter (CD-6 CSX-B model, Mitutoyo, Roissy-en-France, France).

2.5. Experimental design and Statistical analysis

A completely randomized design was applied with three replicates for each PEF processing condition. Where applicable, results were reported as means \pm standard deviations. Differences were evaluated by analysis of variance (ANOVA) and Tukey's test at a 5% significance level using the software *Statistic 13* (StatSoft, USA).

3. Results and Discussion

3.1 Determination of the PEF processing parameters to obtain modified starches with capacity to form stronger hydrogels

In this first part, three different PEF treatment conditions (T1, T2, and T3) set by combining the field strength (E) and energy input (W_T) were evaluated to obtain modified starch with the capacity to form stronger hydrogels, since this was previously associated with better printing performance (Maniglia et al., 2019).

Fig. 2 shows the results of the microscopy analysis on untreated and PEF-treated wheat and cassava starches granules. Cassava starch showed smaller granules with higher variation than wheat starch. Moreover, wheat starches granules showed an almost spherical shape, while cassava starches appeared constituted of round granules with truncated shape (Maniglia, Lima, da Matta Júnior, Oge, et al., 2020; Maniglia, Lima, Matta Junior, Le-Bail, et al., 2020).

PEF did not cause changes or degradation in the cassava starch granule surface and morphology. On the other hand, wheat starch treated by PEF (mainly T2 and T3 conditions) showed some damage and fractures on the granule surfaces. This is consistent with the findings of Zeng et al. (2016), who observed that PEF treatment can promote damage in the outer part of waxy rice starch granules.

Moreover, PEF treatments promoted a slight reduction in the birefringence of cassava starch, thus suggesting possible effects in the granule internal microstructure. Similar effects were not observed for wheat starch. According to Li et al. (2019), PEF can disintegrate the compact starch chains, affecting the surface and inner structures of starch granules to a different extent, depending on the crystalline type of the starch.

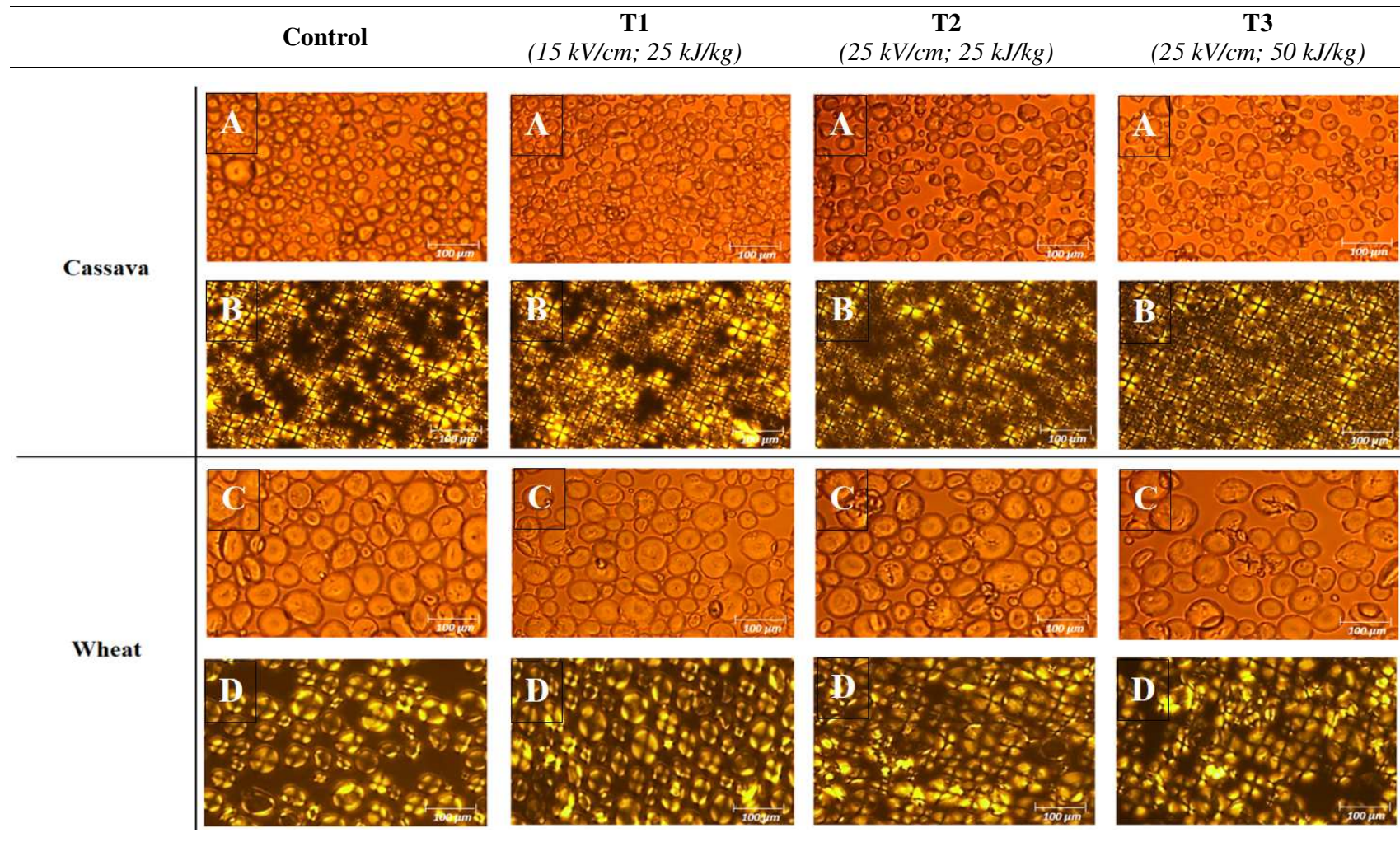


Fig. 2. Optical microscopy (20x magnification) (A, C) and birefringence (B, D) of untreated (control) and PEF-treated cassava and wheat starches.

Fig. 3 shows the pasting profile of cassava and wheat starches, whose parameters are shown in Table 2. In general, as compared with wheat starch, cassava starch showed higher peak apparent viscosity (PAV) and pasting temperature (PT), but lower trough apparent viscosity (TAV) and final apparent viscosity (FAV). In this way, a different behavior in the gelatinization and retrogradation processes should be expected for these two starch sources.

The application of PEF treatment significantly ($p < 0.05$) reduced PAV, independent of processing conditions and starch source. However, it is worth noting that, PEF induced a greater significant reduction in PAV parameter when the extreme treatment conditions (T3) were applied to wheat starch. PAV represents the maximum paste apparent viscosity achieved in the heating stage, and it indicates the exact point between the maximum swelling and the granule rupture (Balet, Guelpa, Fox, & Manley, 2019). Therefore, from our results, it appears that PEF treatment slightly reduced the water-holding capacity of both starches, which, consequently, achieved lower swelling capacity before the disruption. This behavior can be attributed to the fact that PEF may cleave the glycosidic bonds, weakening the starch granules and, consequently, reducing the capacity to maintain their integrity (Chung, Min, Kim, & Lim, 2007). This is consistent with the findings of Duque et al. (2020), who observed that PEF treatment reduced PAV of oat starches and that the effect was more pronounced with increasing specific energy.

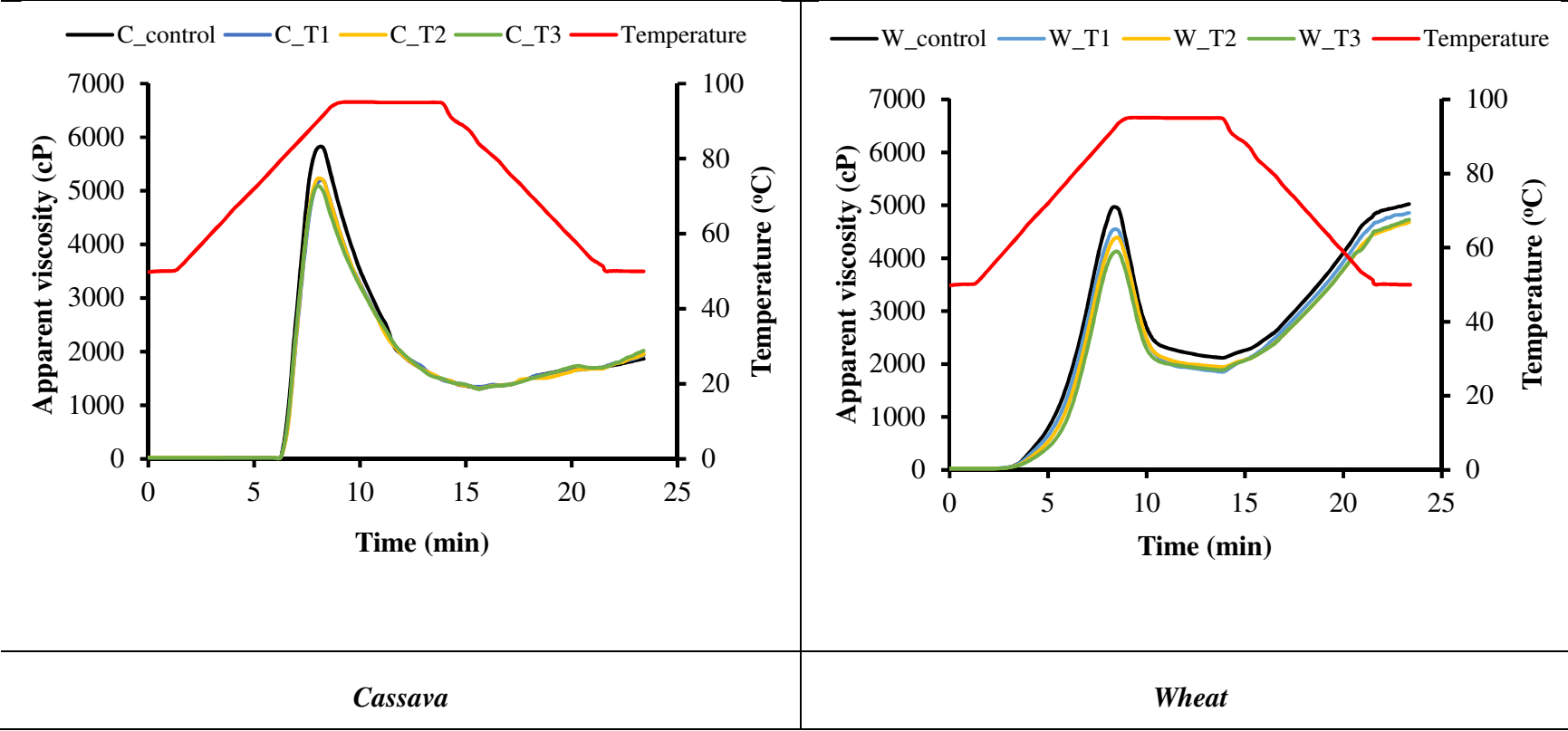
PEF processing did not change the parameters relative breakdown (RBD), final apparent viscosity (FAV), and pasting temperature (PT) of both starches. However, PEF slightly reduced the trough apparent viscosity (TAV) of wheat starch, while inducing no significant ($p > 0.05$) changes in the case of cassava samples. TAV represents the minimum paste apparent viscosity achieved after holding period at the maximum temperature; according to Zou, Xu, Tian, & Li (2019), the reduction of this parameter indicates degradation of crystalline structures and depolymerization (cleavage of glycosidic linkages) promoted by PEF. Additionally, PEF processing significantly ($p < 0.05$) reduced the parameter relative setback (RSB) for cassava starch, while increased the value of this parameter for wheat starch. RSB is a parameter that indicates the trend to retrogradation, which consists of re-association or re-ordering of the starch molecules (Cozzolino, 2016). Therefore, our results indicated that PEF treatment resulted in modified cassava starches with a lower ability to retrograde, while modified wheat starches increased their ability to retrograde especially at the higher treatment intensity investigated. According to Wu et al.

308 (2019), the variations in in the RSB values of starches might be attributed to their changes
309 in molecular structure promoted by the PEF treatment.

310 However, **it is worth mentioning** that only a partial retrogradation takes place during
311 pasting evaluation, being necessary longer periods at lower temperatures for gelling and gel
312 evaluation.

313

314
315



316
317
318

Fig. 3. Pasting profile of untreated (control) and PEF-treated cassava (C) and wheat (W) starches

Table 2. Pasting parameters of untreated (control) and PEF-treated cassava (C) and wheat (W) starches

Samples	PAV (mPa.s)	TAV (mPa.s)	RBD (%)	FAV (mPa.s)	RSB (%)	PT (°C)
C_control	5778.74 ± 120.60 ^a	1381.33 ± 85.47 ^a	75.01 ± 0.85 ^a	1965.67 ± 103.13 ^a	283.28 ± 20.07 ^a	80.43 ± 0.59 ^a
C_T1	5186.33 ± 95.57 ^b	1328.33 ± 34.03 ^a	74.39 ± 0.79 ^a	1922.10 ± 70.72 ^a	245.74 ± 4.60 ^b	80.94 ± 0.53 ^a
C_T2	5091.61 ± 83.96 ^b	1368.67 ± 37.75 ^a	73.12 ± 0.91 ^a	1938.69 ± 94.82 ^a	230.36 ± 9.94 ^b	80.74 ± 0.31 ^a
C_T3	5161.24 ± 116.08 ^b	1360.67 ± 26.95 ^a	73.64 ± 0.80 ^a	1967.11 ± 90.05 ^a	234.75 ± 6.30 ^b	80.55 ± 0.31 ^a
W_control	4955.28 ± 113.72 ^a	2077.80 ± 81.92 ^a	59.48 ± 2.02 ^a	5028.33 ± 95.03 ^a	3.34 ± 0.37 ^d	68.50 ± 1.32 ^a
W_T1	4565.17 ± 82.47 ^b	1853.30 ± 44.55 ^b	59.40 ± 1.65 ^a	4852.67 ± 107.51 ^a	12.75 ± 0.21 ^c	69.17 ± 1.04 ^a
W_T2	4402.52 ± 80.60 ^b	1860.00 ± 61.73 ^b	58.18 ± 2.38 ^a	4727.33 ± 101.02 ^a	16.52 ± 0.58 ^b	67.83 ± 0.76 ^a
W_T3	4093.62 ± 72.97 ^c	1864.10 ± 31.27 ^b	59.89 ± 2.35 ^a	4730.00 ± 89.00 ^a	32.64 ± 0.75 ^a	70.23 ± 1.16 ^a

Results are reported as means ± standard deviation.

Peak Apparent Viscosity (PAV), **Trough** Apparent Viscosity (TAV), Relative Breakdown (RBD), Final Apparent Viscosity (FAV), Relative Setback (RSB), and Pasting Temperature (PT).

a - d: different letters in the same column for each starch source indicates significant difference among samples, as revealed by Tukey's test, $p < 0.05$. $n = 3$.

Fig. 4 shows the hydrogel firmness of untreated (control) and PEF-treated cassava and wheat starches. Results show that hydrogels based on PEF-treated wheat starch showed significantly ($p < 0.05$) higher firmness than that achieved from native starch, while no statistically significant difference was detected between hydrogel based on untreated and PEF-treated cassava starch. Among PEF-treated samples, only the PEF T3 condition (50 kV/cm and 50 kJ/kg) resulted in modified wheat starch with significantly ($p < 0.05$) higher gel firmness, while no significant changes were detected for cassava starch hydrogels regardless the PEF treatment conditions applied. Moreover, it is worth noting that, hydrogels based on wheat starch showed higher firmness than hydrogels based on cassava starch. According to Zhu (2018), differences between the starch sources (crystal pattern, granule size, and molecular structure) may contribute to the local difference in the electric conductivity during the PEF treatment. In addition, the gel formation occurs by the retrogradation process which favors the formation of chain entanglements and the rearrangement of the starch molecules (BeMiller & Whistler, 2009). Moreover, a better gel formation or a higher gel strength in modified starches can be related to better re-association of the starch molecules (amylose and amylopectin)(Lima et al., 2020). In this way, it indicates that PEF treatment promoted formation of starch molecules with better capacity of re-association.

Gel firmness was critical for the next steps of this work. Based on these results, we selected starches modified by PEF with the capacity to form stronger hydrogels. This analysis is a good indication of the printability of the hydrogel and has a good correlation with its behavior when used in real 3D printing (Maniglia et al., 2019). Therefore, in the next steps, we worked with cassava and wheat starches treated by PEF in the T3 condition (50 kV/cm; 50 kJ/kg), as this condition resulted in modified starches with higher hydrogel firmness, at least for one of the starch sources investigated. From now on, the samples C_T3 and W_T3 are named as C_PEF and W_PEF, respectively.

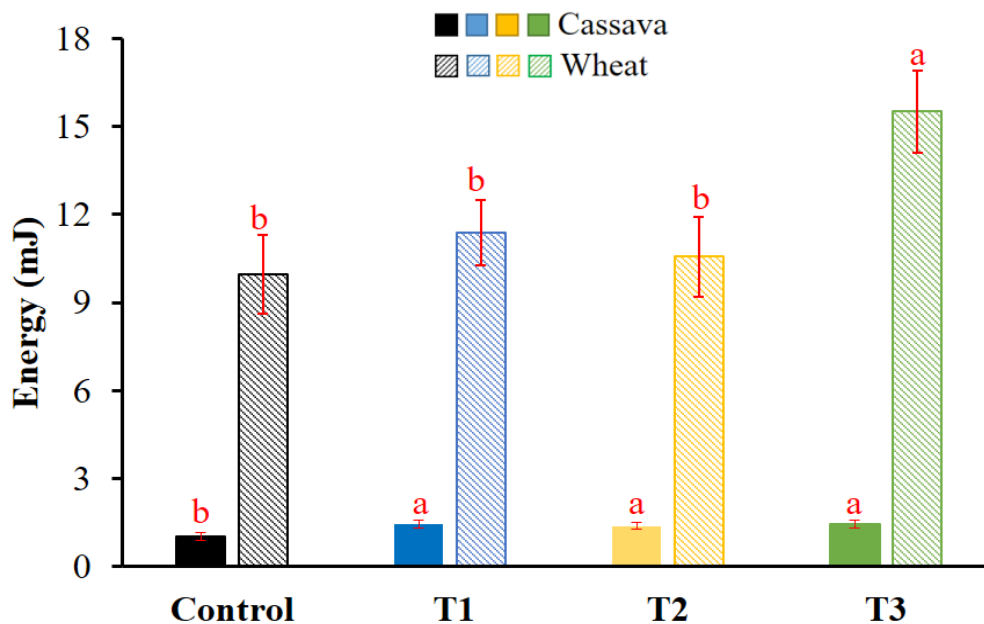


Fig. 4. Hydrogel firmness of untreated (control) and PEF-treated cassava and wheat starches. The red vertical bars are the standard deviations. Different letters above the bars indicate significant differences among the mean values of the starch samples of the same source ($p < 0.05$).

3.2 Characterization of selected PEF modified starches

The selected T3 condition was characterized in relation to the molecular, thermal, and crystalline properties of cassava and wheat starches.

Fig. 5 shows the vibrational spectra of each starch. All samples showed the presence of the same bands at 3300, 2930, 1650, 1350, 1150, 1080, 1040, 1020, 995, and 935 cm^{-1} .

An extremely broadband at 3300 cm^{-1} can be associated with O-H stretching vibrations (Barroso & del Mastro, 2019). The band at 2930 cm^{-1} belongs to C-H bond stretching vibrations (Xiong, Li, Shi, & Ye, 2017). The band at 1650 cm^{-1} was ascribed to H_2O bending vibration, and it arises from the vibrations of adsorbed water molecules in the non-crystalline region (Hong, Chen, Zeng, & Han, 2016; Kizil, Irudayaraj, & Seetharaman, 2002). The band at 1350 cm^{-1} can be attributed to O-H bending due to the primary or secondary alcohols (Muscat, Adhikari, Adhikari, & Chaudhary, 2012).

Starch samples show a fingerprint region based on bands at 1200-900 cm⁻¹ (Fig. 5(B)) and this region provided information about changes in the polymeric structure and conformation of starch (Dankar, Haddarah, Omar, Sepulcre, & Pujola, 2018).

The bands in the fingerprint region are sensitive to changes in starch structure (Warren, Gidley, & Flanagan, 2016). The band around 1040 cm⁻¹ has been linked to ordered structures, the band around 1020 cm⁻¹ to amorphous structures (Lopez-Silva, Bello-Perez, Agama-Acevedo, & Alvarez-Ramirez, 2019). The ratio between the band intensities at 1040 and 1020 cm⁻¹ ($R_{1040/1020}$) can be used as measures of the short-range ordered molecular structure of starch (Flores-Morales, Jiménez-Estrada, & Mora-Escobedo, 2012; Warren et al., 2016). Fig. 5(C) exhibits the estimated ratios $R_{1040/1020}$ between the band intensities of the different starch samples (cassava and wheat control and treated by PEF). The modified starches showed slightly lower ratio $R_{1040/1020}$ when compared with its respective controls. It indicates that PEF treatment affected the degree of short-range order because probably this treatment promoted a reduction in the portion of crystalline structures.

Even so, the results indicate that PEF did not promote modification in the starch functional groups, albeit some alteration in the crystalline portion of granules. In fact, PEF treatment did not change the suspension pH (cassava starch control: 4.90 ± 0.12 , modified cassava starch: 4.76 ± 0.15 , wheat starch control: 5.68 ± 0.10 , modified wheat starch: 5.47 ± 0.14).

Fig. 6 shows the molecular size distribution for the control and modified starches. The first peak consists of molecules of larger size and more ramifications, which can be associated with amylopectins, while the second peak represents molecules of smaller size and a linear structure, which can be associated with amyloses. As expected, wheat and cassava starches show different profiles: wheat starch showed molecular size-fractions more defined (large and small-size), while cassava starch showed a relevant fraction with intermediate-size.

Wheat starch treated by PEF showed a slight reduction of the intermediate-sized molecules, while PEF treatment reduced the larger and intermediate-sized molecules of cassava starch. In this way, in both starch sources, depolymerization was promoted by PEF. Duque et al. (2020) also observed this behavior in oat starches and the authors explained

that it was the reason for the reduction in the peak apparent viscosity (PAV), since the cleavage of glycosidic linkages results in weakening of starch granules and consequently in minor capacity to maintain the granule integrity. The same behavior was observed in our results (Fig. 3), indicating the depolymerization led to easier granule disruption.

Also, the depolymerization promoted by PEF was a determining factor for the formation of stronger gels: the modified starches showed molecular size distribution that resulted in better re-association and packaging, forming a stronger three-dimensional network structure for the hydrogels (Maniglia, Lima, da Matta Júnior, Oge, et al., 2020).

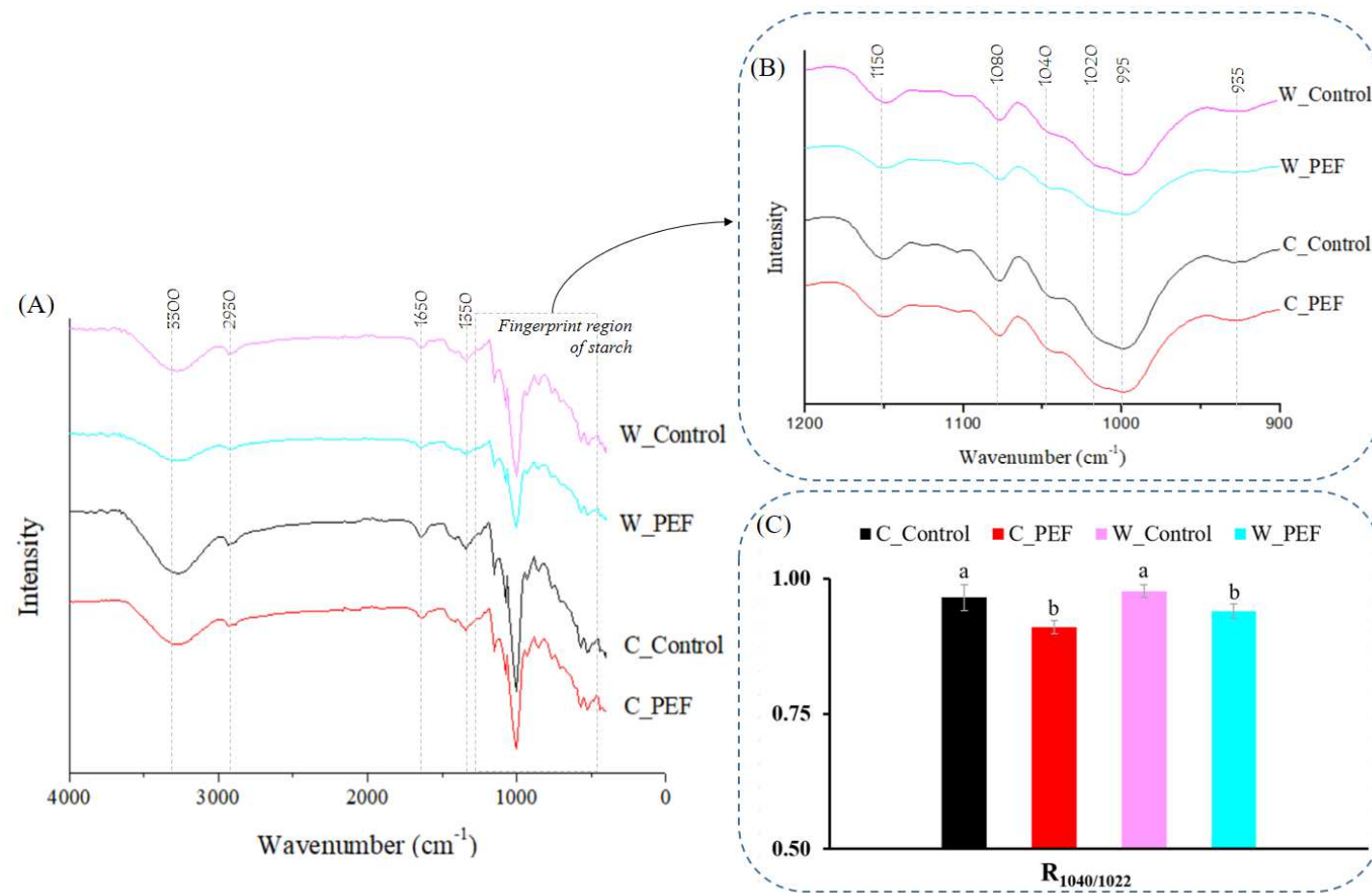


Fig. 5. Vibrational spectra in wavenumber interval between (A) 4000 and 900 cm⁻¹ and between (B) 1200 and 900 cm⁻¹ of the control (W_Control and C_Control) and PEF-treated starches (W_PEF and C_PEF). (C) Estimated ratio ($R_{1040/1020}$) between the band intensities of the different starch samples (untreated and PEF-treated cassava and wheat starch).

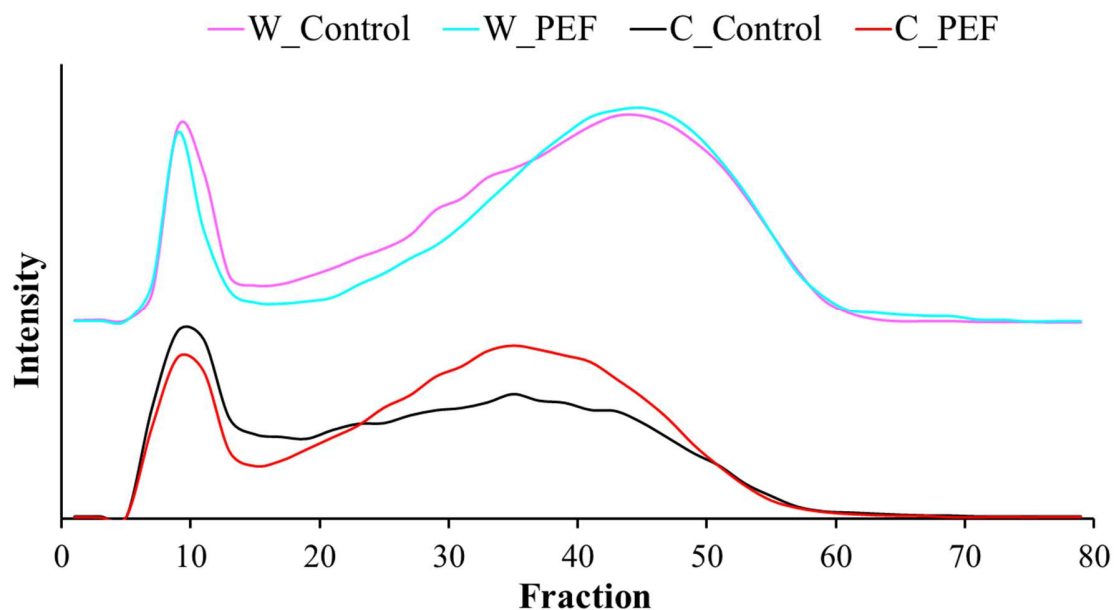


Fig. 6. Molecular size distribution profile (blue value method) of the control (C_Control and W_Control) and modified starches by PEF (C_PEF and W_PEF).

The thermal properties of the wheat and cassava starch gelatinization are shown in Table 3.

Table 3. Gelatinization properties of the control (W_Control and C_Control) and modified starches by PEF (W_PEF and C_PEF) (average \pm standard deviation)

Samples	To (°C)	Tp (°C)	Tf (°C)	ΔH (J/g)
W_Control	48.01 ± 0.32^b	59.85 ± 0.27^c	74.42 ± 0.35^b	9.85 ± 0.12^c
W_PEF	47.73 ± 0.43^b	58.40 ± 0.16^d	73.91 ± 0.43^b	9.15 ± 0.22^d
C_Control	55.79 ± 0.28^a	65.77 ± 0.12^a	81.30 ± 0.23^a	12.80 ± 0.22^a
C_PEF	55.23 ± 0.30^a	64.01 ± 0.26^b	80.85 ± 0.62^a	11.74 ± 0.13^b

a, b: different letters in the same column indicate a significant difference among the samples, as revealed by Tukey's test, $p < 0.05$

To = onset temperature, Tp = peak temperature, Tf = final temperature and ΔH = gelatinization enthalpy.

Both peak temperature (Tp) and gelatinization enthalpy (ΔH) of cassava starch are higher than wheat starch, which indicates cassava starch needs more energy to complete the process of gelatinization than wheat starch. In both starch sources, PEF treatment reduced

the parameters T_p and ΔH . According to Eliasson and Gudmunsson (1996) the gelatinization temperature could be related to the degree of perfection of crystallites, and the gelatinization enthalpy could be related to the degree of crystallinity. Therefore, for better interpretation of these results, XRD analysis was also performed, being the results shown in Fig. 7.

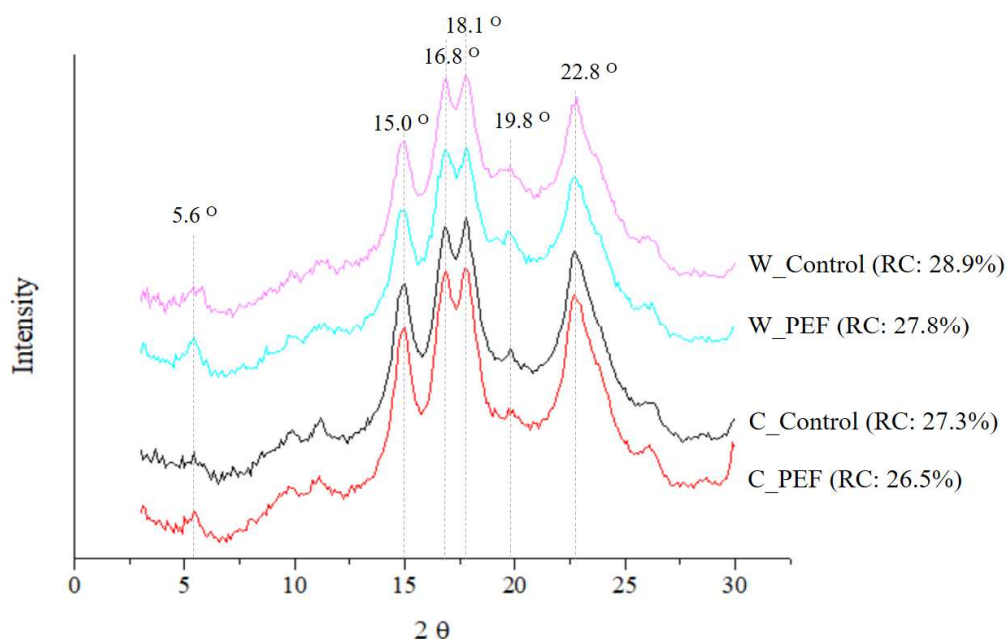


Fig. 7. X-ray powder diffraction patterns of control (W_Control and C_Control) and modified starches by PEF (W_PEF and C_PEF). RC: relative crystallinity.

Results show that the starch samples showed strong singlet peaks (2θ) at 15.0° and 22.8° , unresolved doublet peaks at 16.8° and 18.1° , and small peaks at 5.6° and 19.8° . The evident peaks correspond to typical A-type crystal patterns. The same was observed by Farias et al. (2020) for cassava starch and by Li et al. (2019) for wheat starch.

In addition, we observed that PEF treatment did not alter the crystal patterns, but promoted a slight reduction of the relative crystallinity (RC) of both starch sources. Han et al. (2012) also observed that PEF treatment promoted RC reduction of tapioca starch and the authors discussed that PEF is able to partially destroy the starch crystalline regions by offering higher energy for the interaction between starch granules and water molecules.

In this way, ΔH reduction during gelatinization can be associated with the reduction of crystalline regions. In other words, when starch granules are completely swollen, the

required energy needed to melt the crystalline amylopectin structure and the double helices of amylose was lower in PEF-treated samples when compared to the control starches (Ovando-Martínez, Whitney, Reuhs, Doehlert, & Simsek, 2013).

Given the changes promoted by PEF in starches, in the next item, we will show why these changes improved the printability of the hydrogels based on these starches.

3.3 Potential for 3D printing application: visual aspect, reproducibility, and textural characterization

Fig. 8 shows the printed samples (star, heart, and cylinder-shaped structures) based on hydrogels produced with wheat and cassava starch (control and modified by PEF – treatment T3). Considering wheat starch, PEF resulted in printed samples with a smoother surface, without deformations, when compared with the control. Also, we noted the printed sample with control wheat starch showed a syneresis process, which compromises the integrity of the printed material, while PEF treatment avoided it. It is worth mentioning that these results are very interesting considering the application. On the other hand, PEF treatment did not show visible differences for cassava starch – highlighting the particularity of each source and the need for evaluating them.

Table 4 shows the texture parameters and reproducibility of the printed samples based on control and PEF-treated starches. In general, printed samples based on wheat starches (control and modified) show higher hardness and springiness, lower adhesiveness, cohesiveness, and similar chewiness than cassava starches (control and modified). It indicates that different starch sources result in printed samples with different textures.

Printed samples based on cassava starch (control or modified) hydrogels show higher weight than those produced with wheat starch (control or modified). In addition, by comparing the standard deviation, we observed lower values for the printed samples based on wheat starch hydrogels, indicating that this starch source formed hydrogels more reproducible for 3D printing than cassava starch (lower CV). It can be explained by the superior gel firmness of the wheat starch in comparison to the cassava starch.

Hydrogels based on PEF-treated wheat starch resulted in higher hardness, lower adhesiveness, and similar cohesiveness, springiness, and chewiness than control. Hydrogels based on cassava starch resulted in printed samples with similar texture, considering both

control and PEF treatments. Again, we observed the same PEF treatment promoted an improvement in the printability of wheat starch hydrogels and also changed the texture parameters of the wheat printed samples, whereas, for cassava, the structural changes promoted in starch were not able to improve the hydrogels printability.

Even so, the PEF-treated starches showed no statistical difference in relation to the weight, diameter, and height of their respective control starches, showing similar reproducibility as we can observe by the CV values.

Based on these results we can observe the same PEF treatment resulted in gels with lower apparent viscosity and stronger than the native ones, however, the intensity of the effects of the treatment was more intense for wheat starch than cassava and it also reflected in the 3D printing behavior. Modified cassava starch not showed better performance for 3D printing application than the control, while wheat starch modified by PEF showed superior printability. These results imply that the use of wheat starch can be expanded to industrial applications, such as 3D food printing.

Finally, compared to other green treatments explored by our research group as dry heating and ozone treatments for starch modification focusing on 3D printing application, the emerging PEF treatment showed a lighter effect on the starch properties and consequently in its potential for 3D printing. However, given the advantages of the PEF technique as relative short time, low energy consumption, low temperature, and no production of residues, we consider it is relevant to explore more this technique. For example, a broader investigation into the effect of the PEF process variables may have a more significant effect of this treatment on the starch properties, also considering other starch sources and combinations with other technologies.

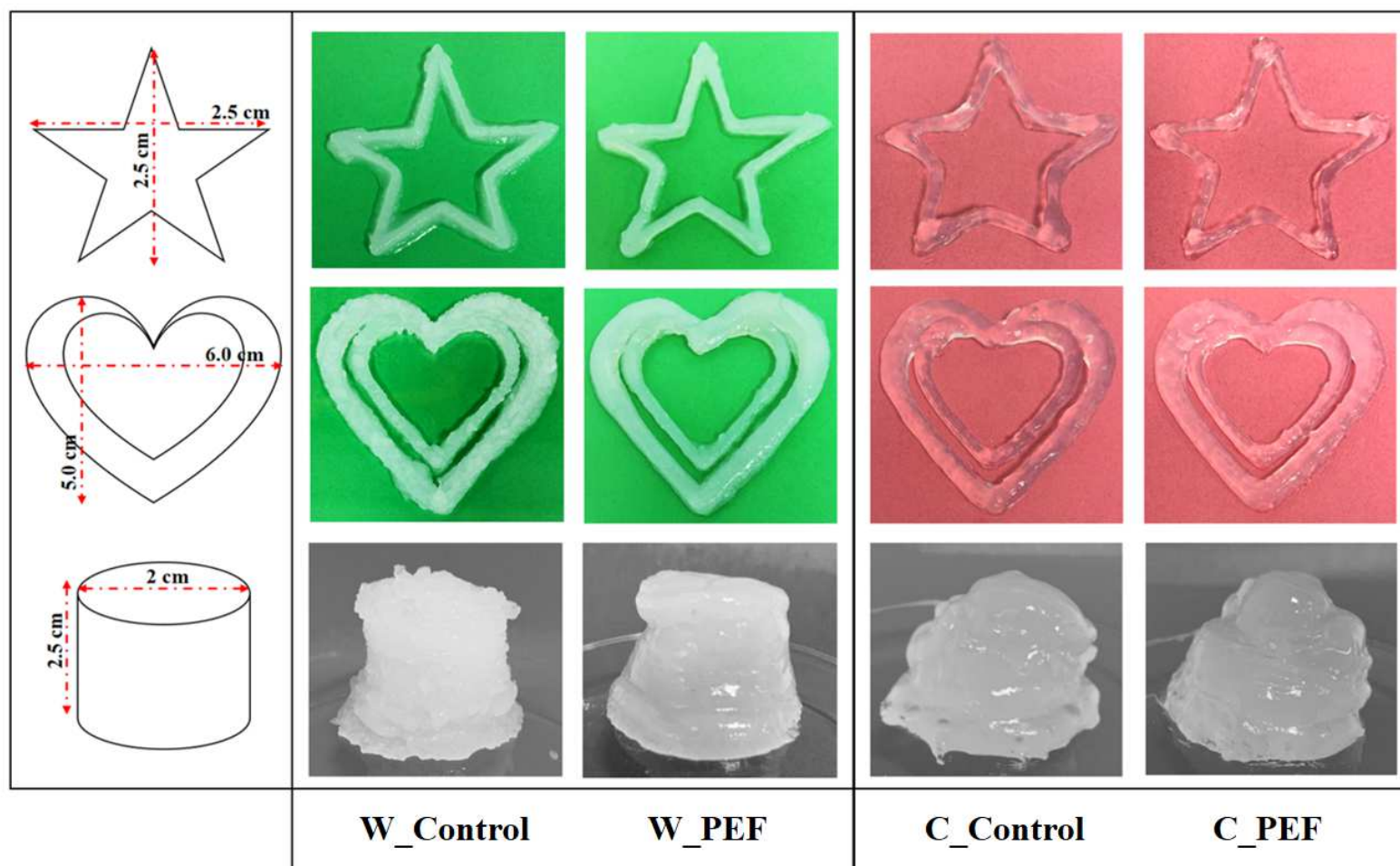


Fig. 8. 3D printed samples (star, heart, and cylinder-shaped structures) based on hydrogels produced with control (W_Control and C_Control) and modified starches by PEF (W_PEF and C_PEF)

506

Table 4. Texture parameters and reproducibility of the printed samples in cylinder shape (average \pm standard deviation)

Hydrogels	Textural parameters					Reproducibility					
	Hardness	Adhesiveness	Cohesiveness	Springiness	Chewiness	Weight		Diameter		Height	
	(N)	(N.s)	(-)	(-)	(-)	W	CV	D	CV	H	CV
						(g)	(%)	(mm)	(%)	(mm)	(%)
W_Control	0.68 \pm 0.08 ^b	-1.67 \pm 0.06 ^b	0.41 \pm 0.01 ^b	0.81 \pm 0.03 ^a	0.27 \pm 0.01 ^a	15.38 \pm 0.21 ^b	1.37	2.50 \pm 0.16 ^a	6.40	2.08 \pm 0.08 ^a	3.85
W_PEF	0.85 \pm 0.05 ^a	-2.01 \pm 0.10 ^c	0.48 \pm 0.06 ^b	0.77 \pm 0.05 ^a	0.30 \pm 0.05 ^a	15.08 \pm 0.13 ^b	0.86	2.45 \pm 0.12 ^a	4.90	2.15 \pm 0.07 ^a	3.26
C_Control	0.33 \pm 0.05 ^c	-0.60 \pm 0.03 ^a	0.57 \pm 0.06 ^a	0.50 \pm 0.05 ^b	0.25 \pm 0.03 ^a	16.07 \pm 0.50 ^a	3.11	2.41 \pm 0.30 ^a	12.45	2.28 \pm 0.21 ^a	9.21
C_PEF	0.39 \pm 0.09 ^c	-0.55 \pm 0.05 ^a	0.64 \pm 0.05 ^a	0.44 \pm 0.03 ^b	0.28 \pm 0.05 ^a	15.89 \pm 0.48 ^a	3.01	2.47 \pm 0.28 ^a	11.34	2.32 \pm 0.25 ^a	10.77

507 a–c: different letters in the same column indicate a significant difference among samples, as revealed by Tukey's test, $p < 0.05$. W:

508 weight, D: diameter, H: height, CV: coefficient of variance.

509

4. Conclusion

This work evaluated for the first time the potential of pulsed electric field (PEF) treatment to enhance starch performance during 3D printing. Two starch sources, wheat and cassava, and three different PEF conditions, varying electric field intensity (E) and total specific energy input (WT), were evaluated.

The three conditions had the same effect on cassava starch (no damage on granules surface, reduction of peak apparent viscosity, firmer gels), while T3 promoted a greater effect on wheat starch (fractures on granules surface, reduction in peak apparent viscosity, and firmer gels). T3 condition was selected for further evaluation, revealing depolymerization, reduction of relative crystallinity, and gelatinization enthalpy, but no changes in functional groups.

Wheat starch treated by PEF resulted in printed samples with a smoother surface and with different texture parameters (higher hardness and lower adhesiveness) when compared with the control starch. However, PEF did not cause changes in the cassava starch, the same behavior observed for modified starch was observed for the control starch (appearance, texture, and reproducibility).

Finally, in this work, we demonstrated that the PEF treatment, an environmentally friendly method, can promote different results depending of the starch source. PEF treatment improved the capacity of wheat starch hydrogels to be used for 3D printing, as well as extending the texture possibilities of printed samples. However, the same was not observed for the cassava starch. Future works are needed to explore more widely different variables of the PEF treatment, or even the combination of PEF with other treatments, thus being able to bring more significant changes in the starch properties.

Declaration of Conflict of Interest

The authors declare that they do not have any competing interests that could have influenced the work behind this publication.

Acknowledgments

The authors are grateful to:

- the Région Pays de la Loire (France) / RFI “FOOD 4 TOMORROW” for funding the Post-doctoral fellowship “STARCH-3D” of BC Maniglia;
- the National Council for Scientific and Technological Development (CNPq, Brazil) for the productivity grant of PED Augusto (306557/2017-7);
- Dr. Manoel D. da Matta Junior, for assistance with the GPC analysis.

References

- Abduh, S. B. M., Leong, S. Y., Agyei, D., & Oey, I. (2019). Understanding the Properties of Starch in Potatoes (*Solanum tuberosum* var. Agria) after Being Treated with Pulsed Electric Field Processing. *Foods*, 8(5), 159. <https://doi.org/10.3390/foods8050159>
- Arnal, Á., Royo, P., Pataro, G., Ferrari, G., Ferreira, V., López-Sabirón, A., & Ferreira, G. (2018). Implementation of PEF Treatment at Real-Scale Tomatoes Processing Considering LCA Methodology as an Innovation Strategy in the Agri-Food Sector. *Sustainability*, 10(4), 979. <https://doi.org/10.3390/su10040979>
- Balet, S., Guelpa, A., Fox, G., & Manley, M. (2019). Rapid Visco Analyser (RVA) as a Tool for Measuring Starch-Related Physicochemical Properties in Cereals: a Review. *Food Analytical Methods*, 12(10), 2344–2360. <https://doi.org/10.1007/s12161-019-01581-w>
- Barroso, A. G., & del Mastro, N. L. (2019). Physicochemical characterization of irradiated arrowroot starch. *Radiation Physics and Chemistry*, 158, 194–198. <https://doi.org/10.1016/j.radphyschem.2019.02.020>
- BeMiller, J. N., & Whistler, R. L. (2009). *Starch: chemistry and technology*. Academic Press.
- Carullo, D., Abera, B. D., Casazza, A. A., Donsì, F., Perego, P., Ferrari, G., & Pataro, G. (2018). Effect of pulsed electric fields and high pressure homogenization on the aqueous extraction of intracellular compounds from the microalgae *Chlorella vulgaris*. *Algal Research*, 31, 60–69. <https://doi.org/10.1016/j.algal.2018.01.017>
- Chung, H.-J., Min, D., Kim, J.-Y., & Lim, S.-T. (2007). Effect of minor addition of xanthan on cross-linking of rice starches by dry heating with phosphate salts. *Journal of*

568 *Applied Polymer Science*, 105(4), 2280–2286. <https://doi.org/10.1002/app.26237>

569 Cozzolino, D. (2016). The use of the rapid visco analyser (RVA) in breeding and selection
570 of cereals. *Journal of Cereal Science*, 70, 282–290.
571 <https://doi.org/10.1016/j.jcs.2016.07.003>

572 Dankar, I., Haddarah, A., Omar, F. E. L., Sepulcre, F., & Pujola, M. (2018). 3D printing
573 technology: The new era for food customization and elaboration. *Trends in Food*
574 *Science & Technology*, 75, 231–242.

575 Duque, S. M. M., Leong, S. Y., Agyei, D., Singh, J., Larsen, N., & Oey, I. (2020).
576 Modifications in the physicochemical properties of flour “fractions” after Pulsed
577 Electric Fields treatment of thermally processed oat. *Innovative Food Science &*
578 *Emerging Technologies*, 64, 102406. <https://doi.org/10.1016/j.ifset.2020.102406>

579 Eliasson, A. C., & Gudmundsson, M. (1996). Starch: Physicochemical and functional
580 aspects. *Food Science And Technology-New York-Marcel Dekker-*, 431–504.

581 Fanli Yang, Min Zhanga, Bhesh Bhandari, Y. L. (2018). Investigation on lemon juice gel as
582 food material for 3D printing and optimization of printing parameters. *LWT - Food*
583 *Science and Technology*, 87, 67–76. <https://doi.org/10.1016/j.lwt.2017.08.054>

584 Farias, F. de A. C., Moretti, M. M. de S., Costa, M. S., BordignonJunior, S. E., Cavalcante,
585 K. B., Boscolo, M., ... Silva, R. da. (2020). Structural and physicochemical
586 characteristics of taioba starch in comparison with cassava starch and its potential for
587 ethanol production. *Industrial Crops and Products*, 157, 112825.
588 <https://doi.org/10.1016/j.indcrop.2020.112825>

589 Flores-Morales, A., Jiménez-Estrada, M., & Mora-Escobedo, R. (2012). Determination of
590 the structural changes by FT-IR, Raman, and CP/MAS ¹³C NMR spectroscopy on
591 retrograded starch of maize tortillas. *Carbohydrate Polymers*, 87(1), 61–68.
592 <https://doi.org/10.1016/j.carbpol.2011.07.011>

593 Giteru, S. G., Oey, I., & Ali, M. A. (2018). Feasibility of using pulsed electric fields to
594 modify biomacromolecules: A review. *Trends in Food Science & Technology*, 72, 91–
595 113. <https://doi.org/10.1016/j.tifs.2017.12.009>

596 Han, Z., Zeng, X. A., Fu, N., Yu, S. J., Chen, X. D., & Kennedy, J. F. (2012). Effects of
597 pulsed electric field treatments on some properties of tapioca starch. *Carbohydrate*
598 *Polymers*, 89(4), 1012–1017. <https://doi.org/10.1016/j.carbpol.2012.02.053>

599 Hong, J., Chen, R., Zeng, X.-A., & Han, Z. (2016). Effect of pulsed electric fields assisted
600 acetylation on morphological, structural and functional characteristics of potato starch.
601 *Food Chemistry*, 192, 15–24. <https://doi.org/10.1016/j.foodchem.2015.06.058>

602 Juliano, B. O. (1971). A simplified assay for milled-rice amylose. *Cereal Science Today*,
603 16, 334–340.

604 Kizil, R., Irudayaraj, J., & Seetharaman, K. (2002). Characterization of irradiated starches
605 by using FT-Raman and FTIR spectroscopy. *Journal of Agricultural and Food*
606 *Chemistry*, 50(14), 3912–3918.

607 Koski, C., & Bose, S. (2019). Effects of Amylose Content on the Mechanical Properties of
608 Starch-Hydroxyapatite 3D Printed Bone Scaffolds. *Additive Manufacturing*, 100817.
609 <https://doi.org/10.1016/j.addma.2019.100817>

610 Li, Q., Wu, Q.-Y., Jiang, W., Qian, J.-Y., Zhang, L., Wu, M., ... Wu, C.-S. (2019). Effect
611 of pulsed electric field on structural properties and digestibility of starches with
612 different crystalline type in solid state. *Carbohydrate Polymers*, 207, 362–370.
613 <https://doi.org/10.1016/j.carbpol.2018.12.001>

614 Lima, D. C., Castanha, N., Maniglia, B. C., Junior, M. D. M., Fuente, C. I. A. La, &
615 Augusto, P. E. D. (2020). Ozone Processing of Cassava Starch. *Ozone: Science &*
616 *Engineering*. <https://doi.org/10.1080/01919512.2020.1756218>

617 Lopez-Silva, M., Bello-Perez, L. A., Agama-Acevedo, E., & Alvarez-Ramirez, J. (2019).
618 Effect of amylose content in morphological, functional and emulsification properties
619 of OSA modified corn starch. *Food Hydrocolloids*, 97, 105212.
620 <https://doi.org/10.1016/j.foodhyd.2019.105212>

621 Maniglia, B. C., Castanha, N., Le-Bail, P., Le-Bail, A., & Augusto, P. E. D. (2020). Starch
622 modification through environmentally friendly alternatives: a review. *Critical Reviews*
623 *in Food Science and Nutrition*, 0(0), 1–24.

624 <https://doi.org/10.1080/10408398.2020.1778633>

625 Maniglia, B. C., Castanha, N., Rojas, M. L., & Augusto, P. E. (2020). Emerging
 626 technologies to enhance starch performance. *Current Opinion in Food Science*.
 627 <https://doi.org/10.1016/j.cofs.2020.09.003>

628 Maniglia, B. C., Lima, D. C., da Matta Júnior, M., Oge, A., Le-Bail, P., Augusto, P. E. D.,
 629 & Le-Bail, A. (2020). Dry heating treatment: A potential tool to improve the wheat
 630 starch properties for 3D food printing application. *Food Research International*, 137,
 631 109731. <https://doi.org/10.1016/j.foodres.2020.109731>

632 Maniglia, B. C., Lima, D. C., Matta Junior, M. D., Le-Bail, P., Le-Bail, A., & Augusto, P.
 633 E. D. (2019). Hydrogels based on ozonated cassava starch: Effect of ozone processing
 634 and gelatinization conditions on enhancing 3D-printing applications. *International*
 635 *Journal of Biological Macromolecules*, 138, 1087–1097.
 636 <https://doi.org/10.1016/j.ijbiomac.2019.07.124>

637 Maniglia, B. C., Lima, D. C., Matta Junior, M. D., Le-Bail, P., Le-Bail, A., & Augusto, P.
 638 E. D. (2020). Preparation of cassava starch hydrogels for application in 3D printing
 639 using dry heating treatment (DHT): A prospective study on the effects of DHT and
 640 gelatinization conditions. *Food Research International*, 128((accepted for
 641 publication)), 108803. <https://doi.org/10.1016/j.foodres.2019.108803>

642 Mantihal, S., Kobun, R., & Lee, B.-B. (2020). 3D food printing of as the new way of
 643 preparing food: A review. *International Journal of Gastronomy and Food Science*, 22,
 644 100260. <https://doi.org/10.1016/j.ijgfs.2020.100260>

645 Muscat, D., Adhikari, B., Adhikari, R., & Chaudhary, D. S. (2012). Comparative study of
 646 film forming behaviour of low and high amylose starches using glycerol and xylitol as
 647 plasticizers. *Journal of Food Engineering*, 109(2), 189–201.
 648 <https://doi.org/10.1016/j.jfoodeng.2011.10.019>

649 Nara, S., & Komiya, T. (1983). Studies on the Relationship Between Water-saturated State
 650 and Crystallinity by the Diffraction Method for Moistened Potato Starch. *Starch -*
 651 *Stärke*, 35(12), 407–410. <https://doi.org/10.1002/star.19830351202>

652 Ovando-Martínez, M., Whitney, K., Reuhs, B. L., Doehlert, D. C., & Simsek, S. (2013).
653 Effect of hydrothermal treatment on physicochemical and digestibility properties of
654 oat starch. *Food Research International*, 52(1), 17–25.
655 <https://doi.org/10.1016/j.foodres.2013.02.035>

656 Postma, P. R., Pataro, G., Capitoli, M., Barbosa, M. J., Wijffels, R. H., Eppink, M. H. M.,
657 ... Ferrari, G. (2016). Selective extraction of intracellular components from the
658 microalga *Chlorella vulgaris* by combined pulsed electric field–temperature treatment.
659 *Bioresource Technology*, 203, 80–88. <https://doi.org/10.1016/j.biortech.2015.12.012>

660 Pourmohammadi, K., Abedi, E., Hashemi, S. M. B., & Torri, L. (2018). Effects of sucrose,
661 isomalt and maltodextrin on microstructural, thermal, pasting and textural properties
662 of wheat and cassava starch gel. *International Journal of Biological Macromolecules*,
663 120, 1935–1943.

664 Raso, J., Frey, W., Ferrari, G., Pataro, G., Knorr, D., Teissie, J., & Miklavčič, D. (2016).
665 Recommendations guidelines on the key information to be reported in studies of
666 application of PEF technology in food and biotechnological processes. *Innovative*
667 *Food Science & Emerging Technologies*, 37, 312–321.
668 <https://doi.org/10.1016/j.ifset.2016.08.003>

669 Shevkani, K., Singh, N., Bajaj, R., & Kaur, A. (2017). Wheat starch production, structure,
670 functionality and applications-a review. *International Journal of Food Science &*
671 *Technology*, 52(1), 38–58. <https://doi.org/10.1111/ijfs.13266>

672 Song, Y., & Jane, J.-L. (2000). Characterization of barley starches of waxy, normal, and
673 high amylose varieties. *Carbohydrate Polymers*, 41(4), 365–377.
674 [https://doi.org/10.1016/S0144-8617\(99\)00098-3](https://doi.org/10.1016/S0144-8617(99)00098-3)

675 Warren, F. J., Gidley, M. J., & Flanagan, B. M. (2016). Infrared spectroscopy as a tool to
676 characterise starch ordered structure—a joint FTIR–ATR, NMR, XRD and DSC
677 study. *Carbohydrate Polymers*, 139, 35–42.

678 Wu, C., Wu, Q.-Y., Wu, M., Jiang, W., Qian, J.-Y., Rao, S.-Q., ... Zhang, C. (2019). Effect
679 of pulsed electric field on properties and multi-scale structure of japonica rice starch.
680 *LWT*, 116, 108515. <https://doi.org/10.1016/j.lwt.2019.108515>

- 681 Xiong, J., Li, Q., Shi, Z., & Ye, J. (2017). Interactions between wheat starch and cellulose
682 derivatives in short-term retrogradation: Rheology and FTIR study. *Food Research*
683 *International*, 100, 858–863.
- 684 Zeng, F., Gao, Q. Y., Han, Z., Zeng, X. A., & Yu, S. J. (2016). Structural properties and
685 digestibility of pulsed electric field treated waxy rice starch. *Food Chemistry*, 194,
686 1313–1319. <https://doi.org/10.1016/j.foodchem.2015.08.104>
- 687 Zhu, F. (2018). Modifications of starch by electric field based techniques. *Trends in Food*
688 *Science and Technology*, 75(November 2017), 158–169.
689 <https://doi.org/10.1016/j.tifs.2018.03.011>
- 690 Zou, J., Xu, M., Tian, J., & Li, B. (2019). Impact of continuous and repeated dry heating
691 treatments on the physicochemical and structural properties of waxy corn starch.
692 *International Journal of Biological Macromolecules*, 135, 379–385.
693 <https://doi.org/10.1016/j.ijbiomac.2019.05.147>